Durability improvement of ancient bricks by cementation of porous media

Paula Lopez-Arce*, David Benavente†, Javier Garcia-Guinea‡,

*****Centro Tecnologico, Departamento de Materiales de Construccion (AITEMIN). 45007, Toledo, Spain.*

†*Laboratorio de Petrologia Aplicada, Unidad Asociada CSIC-Universidad de Alicante. Departamento de CC. de la Tierra y del Medio Ambiente. 03080, Alicante, Spain*

‡*Museo Nacional de Ciencias Naturales (CSIC). 28006, Madrid, Spain.*

Abstract

Time-dependent natural weathering processes suffered by historic bricks in Toledo (Spain) improve their physicomechanical properties by porous infill with gypsum, ettringite and mainly calcite. Both, these bricks and their experimental replica bricks, made from the original calcareous clays fired at the probable historical temperatures (700º - 900ºC), have been analyzed by X-ray diffraction, optical and scanning electron microscopy, mercury intrusion porosimetry and ultrasound velocities to compare pore structure and strength evolution by mineral cementation. The resultant microstructure and mineral fillings depend on brick calcareous composition and firing temperature, the brick location environment, burial, indoor or outdoor walls, the lime-based joint mortars and coat plasters and infiltration waters.

I. Introduction

Toledo City is one of eleven Spanish cities declared by UNESCO as part of "World Heritage". During hundreds of years Toledo was shared by Jewish, Christian and Islamic civilizations producing a well-preserved brick-built architectural-heritage. Today this valuable heritage continues to experience noticeable deterioration, our aim being the preservation and restoration of original materials and to study the causes of changes.

A substantial volume of published work exists[1-4] on decay cases: (i) in diverse building materials with different composition and physical properties, (ii) with different external deterioration agents such as air and

water pollution, moisture, temperature and microorganisms, and (iii) producing dissimilar weathering traces such as salt efflorescence, fissures, falling down of fragments and crust formation.

Salts may be inherent to the brick or mortar, absorbed with groundwater, created by metabolic activity of microorganisms, or formed by reaction with atmospheric pollutants, particularly sulfates, which infiltrate into the brick porosity and bring about precipitation of new phases, e.g., ettringite, thaumasite, mirabilite, gypsum, with a linked crystallization pressure, which produces fissures and cohesion losses.[5-7]

In spite of the usually occurring salt decay, in several cases, under specific conditions the precipitation of calcite or ettringite consolidates the brick or mortar by cementation of surfaces or porous media including reduction of the permeability and increasing of the mechanical resistance.[8-10]

Lime has been used as an essential binder for the production of mortars and plasters since 7000 BC, and both Greeks and Romans were familiar with its use. Traditional or historical lime mortars have been used for masonry structures as joint mortars, as supporting or decorative materials and even as binders for waterproof linings. These were produced before the end of the 19th century, when Portland cement first appeared in building constructions.[11,12] When lime mortars (CaO) are mixed with water they become transformed into calcium hydroxide ($Ca(OH)_2$), the mineral phase also known as slaked lime, hydrated lime or portlandite. The carbonation process in lime mortar is influenced by the diffusion of carbon dioxide into the mortar pore system, following the kinetics of the lime carbonation reaction, by the drying and wetting process in the mortar. All these phenomena depend on the presence of water in the mortar, both in liquid form as well as in vapor and are favored by low temperatures.[13-15] Carbonation does not seem to have a negative influence on the lime mortar performance. In fact, the Romans used long-term aged lime putty achieving excellent lime mortars that have withstood weathering up to the present time. Experimental mortars prepared using traditional aged lime putties (up to 14 years storage under water) show rapid, extensive carbonation, resulting in porosity reduction and ultrasonic speed increase.[16,17] The bricks present an important porosity that induces lime absorption by capillarity and partial carbonation in contact with the interstitial gases, which have a high CO_2 pressure after firing.[18]

The science of materials increasingly focuses on specific details, often safeguarding reactions with the surrounding neighboring materials. Physical properties, composition, chemical reactions and decay mechanisms of brick and mortars have been extensively analyzed in separate studies; conversely not many of the published studies examine mortar-brick interactions.

The excavation and restoration works performed by the Archaeological Service of the Provincial Council of Toledo, for building refurbishements in the City Center have uncovered hitherto concealed structures and bricks providing a wonderful opportunity to collect ancient bricks and mortar samples.

Former studies on these Toledo historical bricks showed unexpectedly high compression strength and low water absorption values. Only a few samples display fissures, high water absorption and low stress compression values.[19]

For comparison purposes, original clays were selected from ancient quarries close to Toledo City Center. In order to measure their physical properties and to assess the mechanical modifications suffered by the true historical brick samples, these experimental fired specimens replicate a comparable original starting point for the ancient Toledo bricks.

The aim of this work is to study the causes of the well preserved status of many ancient bricks of Toledo and to quantify their physicomechanical modifications over time, taking into account cementation processes produced by different weathering mechanisms and the relationships between lime mortars and plasters and these calcareous bricks.

II. Sampling

Toledo is located in the middle of Iberian peninsula; with a continental weather, its main climate characteristics are: long summers and winters and short springs and autumns; dry, with scarce precipitations, and little frequent snow; arid (scarce vegetation and rocky with clayed soils, these, with high thermo-diffusivity and good humidity retention), plentiful sunlight, strongly illuminated in summer, with a tendency to misty in winter; scarce windy, with predominance of West and East winds. The most frequent meteors are hazes, mists and irradiation fogs.[20]

Ancient brick samples were collected from several historical Toledo buildings offering different preservation environments: (i) walls in inner courtyards (brick DIP), (ii) walls in cellars (bricks CG2 and CG3), and (iii) buried walls from archaeological excavations (bricks AL2 and AL3). Table I shows the buildings from which the samples were taken, the estimated age of the bricks according to architectonic style and construction period, original locations, architectonic structures and conservation environments.

The Municipal Record Office of Toledo provided useful data[21] on the original raw clay materials used in the nearby San Bernardo convent zone (SB samples) to the west of the city and also in the chapel of the Concepcion zone (EC samples). The genetic relationships between bricks DIP and AL3 with clays EC, and between bricks AL2, CG2 and CG3 with clays SB were established by XRD, DTA, XRF and EMPA techniques.[22]

In this work we tried simplifying the reproduction of the ancient method of brick manufacture, by hand made elaboration, using brick moulds, with the historical raw clays, but baking the bricks in an electric oven at probable genuine temperatures (700º, 800º and 900ºC, those estimated for the ancient bricks), to make experimental replica bricks for evaluation purposes.

III. Instrumental Methods

The brick samples mineralogy was determined by powder X-ray diffractometry (XRD, Model PW-1710 Philips, Eindhoven, The Netherlands) with CuKα radiation. Patterns were obtained by step scanning from 3º to 75º 2θ with a count of 0.5 s per step, exploration speed of 7º/min and 40 kV and 40 mA in the X-ray tube. The clay mineralogy was also performed by XRD, but the fractions <1.12 μm were obtained from oriented aggregates, swelling in glycerol and heated at 550ºC. A detailed identification of minute amounts of mineral pore infill was also performed by XRD (Model X'Pert PRO MPD, PANalytical, Almelo, Netherlands), with a line focus of 100 microns in diameter, X'Celarator detector, nickel filter without monochromator and sample spinning.

The ancient bricks were analyzed by microscopy methods to study the different types of weathering processes and the cementation of porous media. Thin-section examination was performed under an optical

polarizing microscope (Model Nikon Eclipse C POL 600, Badhoevedorp, The Netherlands), equipped with an automatic photographic system and a digital camera (Model Nikon Coolpix 950). For scanning electron microscopy with energy-dispersive X-ray analysis (SEM-EDS) brick surfaces were coated with gold (20 nm) in a Bio-Rad SC515 sputter coating unit. Model Philips XL20 SEM at accelerating voltages of 20-30 kV and EDS (Model Philips EDAX PV9900 with a light element detector type ECON, Oxford Instrument Analytical, UK) were used for SEM-EDS analysis.

To assess the pore structure evolution of ancient bricks, total porosity and pore size distribution (PSD) of bricks were determined by mercury intrusion porosimetry (MIP) in a radius range of 0.01-110 μm (Model Micromeritics Autopore III S.9400, Norcross, GA).

To evaluate the mechanical strength evolution, the compressional wave velocity, v_P, was obtained using the transmission method, coupling two piezoelectric sensors next to the object at constant pressure. One of the transducers is activated using an ultrasonic pulser and the other is used as a receptor sensor (Model Sonic Viewer-170 OYO). Compressional wave was measured using polarized transducers (500 KHz) (Model Panametrics V101-RB), in which acquired and digitalized waveforms are displayed, manipulated and stored. A visco-elastic couplant was used to achieve good coupling between the transducer and the sample.

IV. Results and Discussion

(1) Mineralogical composition

The XRD analyses of brick samples show their mineralogical composition and hence the significant presence or absence of specific mineralogical phases as firing temperature markers.

Brick DIP displays quartz, feldspar, illite, calcite, gehlenite and hematite. In the polarizing microscope K-feldspar, plagioclase, hematite and low-crystalline calcite were also observed. The diopside absence, which commonly appears in firing process above 900ºC, and the presence of gehlenite and hematite synthesized above 800ºC[23,24] demonstrate that the brick was baked at circa 900ºC and not above. XRD analyses showed that bricks CG2 and CG3 display quartz, feldspar, illite, calcite and gehlenite. In the polarizing microscope altered K-feldspar and plagioclase and calcite negative crystals, hematite and low-crystalline calcite grains

can also be observed. The diopside absence and the presence of gehlenite traces demonstrate that these bricks were fired a bit over 800ºC. Bricks AL2 and AL3 showed quartz, feldspar, calcite, dolomite and illite by analyzing XRD data. In the polarizing microscope, altered K-feldspar and plagioclase, garnets and many primary grains of calcite and biotite and muscovite megacrysts in matrix were observed. The absence of high temperature phases and the presence of calcite and dolomite in these bricks, point to firing temperatures circa 700ºC.[25]

The SB4 clay powder displays 14% quartz, 10% feldspar, 16% calcite, 7% dolomite and 56% phyllosilicates; the XRD analyses of the oriented aggregates show that phyllosilicates are mainly illite with traces of kaolinite. The EC6 clay case displays 8% quartz, 24% feldspar, 11% calcite, 10% dolomite and 47% phyllosilicates; the oriented aggregates show 14% smectite, 22% illite and 11% kaolinite. Firing these clay samples at the probable genuine temperatures (700º, 800º and 900ºC), the same high temperature phases detected in the historical bricks become visible, which suggest an approximate selection and source origin. The comparison among physicomechanical properties must be performed between: (i) brick-DIP and clay-EC6 fired at 900ºC (EC6-900), (ii) brick-AL3 and clay- EC6 fired at 700ºC (EC6-700), (iii) bricks-CG2 and CG3 and clay-SB4 fired at 800ºC (SB4-800), and (iv) brick-AL2 and clay-SB4 fired at 700ºC (SB4-700).[22]

(2) Porous media evolution

The progressive cementation of the porous system was qualitatively studied by POM and SEM and quantitatively by MIP in the pore radius interval from 0.001 μm to 110 μm. Porosity is defined as the ratio of the volume of voids to total volume of brick, expressed as a percentage. This is linked to the flow of weathering agents and the remaining moisture produces a negative influence on brick durability. All ancient bricks of Toledo analyzed showed reduction in overall porosity ranging from 2.1% to 11.2%.

Burial AL2 and AL3 bricks, fired below 700ºC, display neo-formed calcite crystals in the porosity media and diluted and corroded primary calcite grains in the clay-stone matrix. These calcites were not dissociated in the brick firing and they could be a possible calcium carbonate source for the neo-formed crystals. In these bricks, calcite crystals display different textures that could depend on the acidity and flow rate of solutions

that react with the mineral composition. Soft surfaces with no sharp crystals suggest a dissolution process by the interaction of calcite crystals with lightly acid solutions and a slow flow rate. While rough surfaces with cavities suggest a corrosion process by interaction with higher acid solutions under energetic flow rates, that cause both dissolution and corrosion processes. Neo-crystallization is produced from the dissolution of calcite crystals causing deposition in the pore system, giving rise to new calcite crystals with druses crystallizations of slabs and needles, sometimes with chaotic spatial orientation, which can be interpreted by different flowing directions during the crystallization.[26] A mechanistic validation of these different textures can be observed in Fig.1.

Figure 1a illustrates the three processes of dissolution, corrosion and neo-crystallization in the AL3 brick. Figures 1b, 1c and 1d display, at different scales, the same processes in the AL2 brick; the final result being pores filled with calcite crystals; for AL3 they measure from 0.3 to 3 μm, and in the AL2 case, from 30 to 110 μm.

Comparative mercury porosimetry analyses between the ancient AL3 brick and its experimental replica EC6-M7 (Table II) showed the pore size distribution (PSD) evolution as follows: (i) an almost constant percentage of pores with a radius in the range 31.6-110 μm, (ii) a 14.96% drop of 0.316-3.16 μm pores, and (iii) a 15.07% increase of pores with radius <0.316 μm (Fig.2). This could be produced by corrosion of infiltration fluids; whereas 0.316-3.16 pores could be cemented by $CaCO_3$ saturated solutions derived from primary calcite dissolution or from the outer cover of the carbonated lime mortar. The calcium hydroxide coating combined with the presence of large pores makes this region vulnerable to chemical attack, increasing the permeability and serving as channels for solution access.[27]

The ancient AL2 brick and its experimental replica SB4-M7 (Table II) showed the PSD evolution as follows: (i) an almost constant percentage of pores with a radius in the range 31.6-110 μm, (ii) a 26.46% drop of 0.316-3.16 μm pores, and (iii) a 25.43% increase of pores with radius <0.316 μm (Fig.2).

The larger pore sizes of AL2 brick in respect to AL3 brick could be linked with the grain size of their raw clays (SB4 and EC6, respectively), hand-kneading and different percentage of gravel and sand ratios (Table

III). In this specific AL2 brick, the additional possible cause of the larger pores formation coupled with CO_2 emissions was not possible because it does not reach 700ºC during the brick firing. Most of the porosity observed before 800ºC depends on the type of clay, the size and concentration of the inclusions, the organic matter and volatiles.[28]

Figures 4a and 4b illustrate two different types of cementation in AL2 brick: fissures filled with calcite neo-formed crystals and gypsum in pores precipitated by solutions coming from the mortar or the surrounding groundwater (see sketch in Fig. 5c). Furthermore, percolation waters can enhance their acidification through soil enriched in CO_2 by organic matter (algae and bacteria) where the bricks were buried[19], migrating through the pore structure of the ceramic body and attacking the silicate phases of the brick. This may explain the corrosion pits and the porosity <0.316 μm generated.

The CG3 brick shows large amounts of gypsum in the pore system; the joint mortar originally was lime-mortar with arkose aggregate but nowadays it encloses rather neo-formed calcite and gypsum. The gypsum could stem from numerous sources;[29] in this case, it is essential to explain that CG3 brick was collected from a wall in a cellar placed below the Greco residence gardens. A possible gypsum source could have been the reactions between Na-Mg sulfates from the brick or from the infiltration waters with the lime mortar or the hydrous calcium silicates (CSH) of mortars, or a mixture of sources (Fig. 5b). The role of atmospheric pollution as a source of SO_2 could be discarded, because Toledo City does not exceed the threshold value for the SO_2, estimated in 500 mg/m^3, according to the directive 30/1999/CE. In fact, the normal value for this component it is about 4-5 mg/m^3. The average analytical data from Tagus river waters in Torcon, Guajaraz and Castrejon reservoirs, between 1987-1996, illustrates on the sulfates content in Toledo groundwaters, and its possible contribution in the sulfatation processes (Table IV).

The dissolution of the mortar and its infiltration into the brick has produced the precipitation of gypsum crystals in fissures and pores (Fig. 4c). Under the optical microscope, the mortar in the boundary shows large crystals (1 mm) of fissured quartz and neo-formed crystals of calcite and gypsum and visible amorphous veins from mortar towards the core of the brick matrix; the infiltration veins were identified as calcium sulfate (gypsum) using SEM –EDS.

Pore size distribution in CG3 brick (Table II) is as follows: (i) a slight increase of 2.79% of pores with a radius in the range 31.6-110 μm, (ii) a 28.96% drop of 0.316-3.16 μm pores, and (iii) a 26.63% increase of pores with radius <0.316 μm (Fig. 3). This can be attributed to the intrinsic growth of gypsum as intergrowth and interlocking crystals performing a microporous bed[30] that seals the 0.316-3.16 μm pores but generates the pores <0.316 μm.

In the CG2 brick case, we observe ettringite [$Ca_6Al_2(SO_4)_3(OH)_{12}\cdot 26(H_2O)$] in pores with larger sizes than the pores studied by SEM in other samples, e.g., Figure 5a shows an infiltrated pore with a probable solution from lime-gypsum mortar and/or plaster used as coat for the external wall. The environmental conditions (~1 atm), hypogeal temperature (from 15ºC to 18ºC) and humidity of the residence of El Greco cellar facilitate the crystallization and conservation of these fragile needle ettringite crystals that have formed a closed network filling up many pores (Figs. 6a and 6b).

The analyses of the pore size distribution evolution in CG2 brick (Table II) is as follows: (i) a slight drop of 0.66% of pores with a radius in the range 31.6-110 μm, (ii) a 42.15% decrease of 0.316-3.16 μm pores, (iii) a 44.57% increase of pores with radius <0.316 μm (Fig. 3). This pore reduction, detected by PSD, could be explained by calcite cementation in the pore system. Later ettringite formation in large sized pores are only localized close the outer surface of the CG2 brick (~1 cm) and it can be linked with the lime-sulfate joint mortar and the coat plaster in a hypogeal environment. The excellence of the highly hydrated ettringite needles observed by SEM (Fig. 6b), the plane-zoned distribution of the ettringite, the hypogeal environment and the calcite amount rising (Fig. 5b) towards the core of the brick are in good agreement with this proposed genesis. The increase of pore with radius <0.316 μm can be explained by the ettringite needles that seal macropores but generate a microporous network. The XRD analyses with a focused beam of the whitish needles in CG2 macro-pores show pure ettringite. This primary ettringite is not unavoidably negative, it can help the cementation, acting as a strong and durable binder[9,31]. Ettringite expansion depends mainly on the positions where ettringite crystals form. In a pore solution of high alkalinity, ettringite crystals form in situ and cause a large expansion. Alternately, they precipitate partially or completely in voids and macropores,

hence giving rise to a little expansion or no expansion.[32,33] This fact explains the low damage produced by ettringite crystallization in macropores of the studied bricks.

Using polarizing microscopy, brick DIP displays calcite pheno-crystals with low crystallinity and calcite micro-grains dispersed in the matrix. These were generated by environmental re-carbonation of the CaO grains formed during brick firing up to 900ºC in accordance with the well-know steps of $Ca(OH)_2$ and atmospheric CO_2 reactions (Fig. 4d). The carbonation of lime takes place via the transformation of portlandite to calcite. This is a two-stage process. First, carbon dioxide dissolves in water. Second, calcium hydroxide reacts with the carbonic acid in solution (Fig. 5a).[11]

The pore size distribution evolution in DIP brick (Table II) is as follows: (i) an almost constant percentage (only a 0.89% drop) of pores with a radius in the range 31.6-110 μm, (ii) a strong drop of 41.68% of 0.316-3.16 μm pores due to re-carbonation, and (iii) a large increase of 42.96% of pores with radius <0.316 μm (Fig. 3). The small $Ca(OH)_2$ particle size in a long-term aged putty enhances dissolution and increases the saturation degree creating a higher volume of pores with r<0.1μm. These small pores can sustain very high super-saturation degree with respect to $CaCO_3$, resulting in high nucleation rates.[34]

(3) Mechanical properties evolution

Table V illustrates the comparative results of physicomechanical properties of ancient bricks and the historical raw clays fired at the probable genuine temperature ranges (700º, 800º and 900ºC) as experimental replica bricks.

To asses the balance between dissolution (weight loss) and precipitation (weight gain), the bulk density of samples have been calculated. The results, compiled in Table V, suggest an equilibrium between dissolution and precipitation of minerals, because density keeps almost constant in all the studied samples, in both ancient and experimental replica bricks. Only a little gain (0.1 g/cm^3) is produced in the ancient bricks, probably caused by new mineral precipitation.

The strength of the brick is an essential parameter in determining its durability as is the material's resistance to the action of several important decay mechanisms such as frost and salt action as well as

capillary pressure during the wetting and drying cycles.[35] Bricks with high compression strength, Young's module or ultrasonic wave propagation velocities have an increased durability.[36]

Compressional velocities of the mechanical evolution linked to the cementation process are measured in both ancient and experimental replica bricks. During carbonation, pores are filled by calcite. As a result, the brick-forming mineral content is changing and mechanical properties improved by porosity reduction and cementation grade increase. This fact is reflected in increased v_P values after cementation, because compressional velocities of calcite (6.65 km/s) are higher than in clay minerals (1.8-2.4 km/s)[37] and the pore space is reduced by calcite precipitation.

The ultrasonic measurements in the analyzed ancient bricks demonstrate that in all cases the v_P values increase (between 0.28 to 1.55 km/s) for pore cementation with gypsum (AL2, CG3), calcite (AL2, AL3, CG2, CG3, DIP) or calcite-ettringite (CG2).

Brick strength is calculated using a destructive laboratory uniaxial compressive testing on a prepared sample, determining the maximum value of stress attained before failure in order to evaluate the brick mechanical quality. The uniaxial compressive strength depends heavily on microstructural factors such as pores and fractures, grain size, degree of cementation and the elastic properties of brick-forming minerals.[38] Another test used to measure material strength is the study of ultrasonic waves, a non destructive measurement, and therefore, suitable for historic samples. The most used ultrasonic parameter in material strength determination is the compressional wave velocity (v_P), since they are closely linked to microstructural factors.[37,39]

Using different correlations between uniaxial compressive strength and compressional velocity for this kind of materials,[40,41] the variation of compressive strength, $\Delta\sigma_C$, with the compressional velocity, Δv_P, may be estimated as: $\Delta\sigma_C$ (MPa) ~ 14 Δv_P (km/s). From this correlation, the improvement of compressive strength by the cementation process in the ancient bricks may be established between 3.94 and 21.68 MPa (Table V).

V. Conclusions

The analyses of the physicomechanical properties of historical bricks in Toledo and experimental replica bricks made with historical clays collected from the original quarries near Toledo City and fired within the probable genuine temperature ranges (700º, 800º and 900ºC) have been evaluated. These ancient calcareous bricks showed a total porosity reduction from 2.1 to 11.2%, an increase of v_P ultrasonic values from 0.28 to 1.55 km/s, and compression strength between 3.94 and 21.68 MPa. The evaluation of pore size distribution evolution shows a 15%-43% decrease of pores with a radius in the range 0.316-3.16 μm, due to calcite and gypsum cementation, that corresponds with a 15%-45% increase of pores with radii smaller than 0.316 μm, due to brick corrosion or microporous network generated by gypsum and ettringite precipitation.

Brick durability is mainly influenced by both pore structure and material strength and an increased degree of cementation results in greater mechanical strength (compressional velocity and uniaxial compressive strength) and lower total porosity. The unusual time-dependent improvement of the brick physicomechanical properties is associated with the porous system cementation as follows:

(i) ~15% to 26% in buried bricks originally fired up to 700ºC: re-precipitation of calcite crystals from dissolution and corrosion of primary calcite grains,

(ii) ~30% in buried bricks fired circa 700ºC and bricks taken from cellars and fired circa 800ºC: precipitation of calcite and gypsum crystals from dissolution of the carbonated-sulfated joint mortar.

(iii) ~42% in bricks also taken from indoor walls placed in cellars and fired circa 800ºC: precipitation of calcite and ettringite crystals from dissolution of the carbonated-sulfated joint mortar.

(iv) ~43% in bricks taken from outdoor walls and fired circa 900ºC: hydration-recarbonation of the CaO grains inside the brick matrix by environmental water and CO_2 reaction.

The obtained results demonstrate that weathering processes do not automatically produce decay of building materials; in contrast, they can improve durability.

Acknowledgements

Authors are especially indebted to Josefo Bedoya and Laura Tormo, technicians of the ESEM-EDS-WDS microscope of the Museo Nacional de Ciencias Naturales (Madrid). Thanks to L. Garcia-Cuartero (Aguas Toledo, S.A) and C. Triviño (Lab. of Toledo City) for help us with the chemical analysis of waters from Castrejon, Torcon and Guajaraz reservoirs and Tagus River. We are also grateful to Juan Manuel Rojas Malo, the archaeologist who helps us with the sampling and archaeological documentation. Thanks to Rafael Gonzalez Martin and Emilio Matesanz for the accurate XRD analyses, and we also thanks to George Burland for the English review of the manuscript.

References

[1]X. Ariño, A. Gomez-Bolea and C. Saiz-Jimenez, "Lichens on Ancient Mortars," *Int. Biodeter. Biodegr.*, **40** [2 4], 217-24 (1997).

[2]S.W. Massey, "The effects of ozone and NO_x on the deterioration of calcareous stone," *Sci. Total Environ.*, **227**, 109-21 (1999).

[3]G. Cultrone, M.J. De La Torre, E.M. Sebastian, O. Cazalla and C. Rodriguez-Navarro, "Behavior of brick samples in aggressive environments," *Water Air Soil Poll.*, **119**, 191-207 (2000).

[4]D. Mottershead, A. Gorbushina, G. Lucas and J. Wright, "The influence of marine salts, aspect and microbes in the weathering of sandstone in two historic structures," *Build. Environ.*, **38** [9-10] 1193-1204 (2003).

[5]N.J. Crammond, "The thaumasite form of sulfate attack in the UK," *Cement Concrete Comp.*, **25**, 809-18 (2003).

[6]H. Böke and A. Sedat, "Ettringite formation in historic bath brick-lime plasters," *Cement Concrete Res.*, **33**, 1457-64 (2003).

[7]G.W. Scherer, "Stress from crystallization of salt," *Cement Concrete Res.*, **34**, 1613-24 (2004).

[8]A. Török, "Surface strength and mineralogy of weathering crust on limestone buildings in Budapest," *Build. Environ.*, **38** [9-10] 1185-92 (2003).

[9]F.P. Glasser, L. Zhang and Q. Zhou, "Reactions of aluminate cements with calcium sulfate"; pp.551-64 in *International Conference on Calcium Aluminate Cements (CAC),* Inst Mat, Cerman Div, Cement & Concrete Grp., Soc. Chem. Ind., Construct Mat Grp., IOM Communicat. Ltd. Heriot-Watt Univ., Edinburgh, Scotland, Jul. 16-19, 2001.

[10]F. Rassineux, J.C. Petit and A. Meunier, "Ancient analogues of modern cement - Calcium Hydrosilicates in mortars and concretes from Gallo-Roman thermal baths of western France," *J. Am. Ceram. Soc.*, **72** [6] 1026-32 (1989).

[11]A. Moropoulou, K. Polikreti, A. Bakolas and E. Aggelakopoulou, "The effects of limestone characteristics and calcinations temperature to the reactivity of the quicklime," *Cement Concrete Res*., **31**, 633-39 (2001).

[12]A. Moropoulou, K. Polikreti, A. Bakolas and P. Michailidis, "Correlation of physicochemical and mechanical properties of historical mortars and classification by multivariate statistics," *Cement Concrete Res*., **33**, 891-98 (2003).

[13]K. Vanbalen and D. Vangemert, "Modeling lime mortar carbonation," *Mater. Struct*., **27** [171] 393-98 (1994).

[14]S. Sanchez-Moral, J. Garcia-Guinea, L. Luque, R. Gonzalez-Martin and P. Lopez-Arce, "Carbonation kinetics in roman-like lime mortars," *Mater. Construcc*., **54** [275] 23-36 (2004).

[15]J.F. Young, RL. Berger and J. Breese, "Accelerated curing of compacted calcium silicate mortars on exposure to CO_2," *J. Am. Ceram. Soc*., **57** [9] 394-97 (1974).

[16]O. Cazalla, C. Rodriguez-Navarro, E. Sebastian, G. Cultrone and M.J. De la Torre, "Aging of lime putty: Effects on traditional lime mortar carbonation," *J. Am. Ceram. Soc*., **83** [5] 1070-76 (2000).

[17]C. Rodriguez-Navarro, E. Hansen and WS. Ginell, "Calcium hydroxide crystal evolution upon aging of lime putty" *J. Am. Ceram. Soc*., **81** [11] 3032-34 (1998).

[18]E. Donath, "The Chemistry of Tiles and Bricks Industry," (in Ger.), *Sammlung Chemischer und Chemisch-Technisher Varträge,* **30** [5-6] 153-226 (1928).

[19]P. Lopez-Arce and J. Garcia-Guinea, "Weathering traces in ancient bricks from historic buildings," *Build. Environ., in press*.

[20]F. Aranda-Alonso, F. Aranda Gutierrez, M. Aranda Gutierrez, "Observaciones sobre el clima de Toledo" ("Observations on Toledo climate"); Instituto Provincial de Investigaciones - Estudios Toledanos and Instituto de Edafología y Biología Vegetal (CSIC). *Ciencia y Técnica Toledanas*, Toledo, Spain, S. VIII, **2**, 1984.

[21]M.A. Marichalar, Nueva Signatura [2330], *Archivo Municipal de Toledo (AMT)*, Toledo, Spain, 1825.

[22]P. Lopez-Arce, “Ladrillos de edificios históricos de Toledo: Caracterización, origen de las materias primas y aplicaciones para su preservación y conservación” (“Bricks from historic buildings: Characterization, origing or raw materials and applications for its preservation and restoration”); *Ph.D. Thesis. Universidad Complutense de Madrid,* Spain, 2004.

[23]E. Barahona, “Arcillas de ladrillería de la provincia de Granada: evaluación de algunos ensayos de materias primas” (“Brick clays from the Granada province: evaluation of some tests of raw materials”); *Ph.D. Thesis*, *Universidad de Granada, Spain,* 1974.

[24]F. Veniale, “Modern Techniques of Analysis Applied to Ancient Ceramics”; pp. 141-66 in *Advanced Workshop on Analytical Methodologies for the investigation of Damaged stones*” (Pavia, Italy, 1990). Edited by F. Veniale and U. Zezza. La Goliardica Pavese, Pavia, Italy, 1990.

[25]R.S. Boynton, “Chemistry and Technology of Lime and Limestone,” 2nd ed., Wiley, New York, 1980.

[26]P. Lopez-Arce, J. Garcia-Guinea, M. Gracia, J. Obis, “Bricks in historical buildings of Toledo City: characterisation and restoration,” *Mater. Charact.*, **50**, 59-68 (2003).

[27]D. Bonen, “Calcium hydroxide deposition in the near interfacial zone in plain concrete,” *J. Am. Ceram. Soc*., **77** [1] 193-96 (1994).

[28]M.S. Tite and Y. Maniatis, “Scanning Electron Microscopy of Fired Calcareous Clays,” *Trans. J. Br. Ceram. Soc.*, **74**, 19-22 (1975).

[29]M. Collepardi, “Thaumasite formation and deterioration in historic buildings,” *Cement Concrete Comp.*, **21**, 147-54 (1999).

[30]I. Soroka and P.J. Sereda, “Interrelation of hardness modulus of elasticity and porosity in various gypsum systems,” *J. Am. Ceram. Soc*., **51** [6] 337-40 (1968).

[31]M. Collepardi, “A state-of-the-art review on delayed ettringite attack on concrete,” *Cement Concrete Res.*, **25**, 401-07 (2003).

[32]G.W. Scherer, “Factors affecting crystallization pressure,” in *Internal Sulfate Attack: Proceedings of RILEM Workshop on Delayed Ettringite Formation*. Edited by K.L. Scrivener and J. Scrivener. RILEM Publications, Paris, 2004.

[33]D. Min and T. Mingshu, "Formation and expansion of ettringite crystals," *Cement Concrete Res*., **24** [1] 119-26 (1994).

[34]C. Rodriguez-Navarro, O. Cazalla, K. Elert and E. Sebastian, "Liesegang pattern development in carbonating traditional lime mortars," *Proc. R. Soc. Lond. A.,* **458**, 2261-73 (2002).

[35]D. Benavente, M.A. Garcia del Cura, R. Fort and S. Ordoñez, "Durability estimation of porous building stones from pore structure and strength," *Eng. Geol.*, **74**, 113-27 (2004).

[36]K. Elert, G. Cultrone, C. Rodriguez-Navarro and E.Sebastian, "Durability of bricks used in the conservation of historic buildings influence of composition and microstructure," *J. Cult. Herit*., **4**, 91-99 (2003).

[37]N.I. Christens, "Seismic Velocities"; pp. 429-546 in *Practical handbook of physical properties of rocks and minerals*. Edited by RS. Carmichael, Boca Raton: CRC Press, 1990.

[38]R.E. Goodman, "Introduction to rock mechanics". Edited by John Wiley & Sons, New York, 1989.

[39]J.H. Schön, "Physical properties of rocks: fundamentals and principles of petrophysics," in *Handbook of geophysical exploration*. Edited by Pergamon, Section I, Vol. 18, Seismic Exploration, New York, 1996.

[40]G. Cultrone, E. Sebastian, O. Cazalla, M. Nehcar, R. Romero and M.G. Bagur, "Ultrasound and mechanical tests combined with ANOVA to evaluate brick quality," *Ceram. Int*., **27** [4] 401-06 (2001).

[41]G. Cultrone, E. Sebastian and M. J. de la Torre, "Mineralogical and physical behaviour of solid bricks with additives," *Constr. Build. Mater*., **19** [1] 39-48 (2005).

Footnotes

"This work is based in part on the thesis submitted by P. Lopez-Arce for the ph.D in Geology, Complutense University of Madrid, Spain, 2004."

"Supported by the Plan Nacional de I+D CICYT 1FD, Grant No. 1997-0561 (Spain) and the CICYT-JCCM (agreement 2002-2004) (Spain)."

Figure Captions

Fig. 1. SEM photomicrographs of AL3 (a) and AL2 (b,c,d) bricks showing calcite dissolution-corrosion and re-crystallization inside their pores.

Fig. 2. Accumulative mercury intrusion and pore size distribution curves of ancient bricks from burial environments and experimental replica bricks.

Fig. 3. Accumulative mercury intrusion and pore size distribution curves of ancient bricks from aerial environments and experimental replica bricks.

Fig. 4. POM images of: (a) fissure and pore filled with calcite crystals in AL2 brick and (d) recarbonation of CaO grains in DIP brick; SEM images of: (b) pore filled with gypsum crystals in AL2 brick and (c) joint mortar filtration inside fissures of CG3 brick.

Fig. 5. Carbonation and sulfation processes of mortars and re-crystallization of calcite, gypsum and ettringite in the studied brick walls.

Fig. 6. SEM photomicrographs of ettringite crystals in pores of CG2 brick. (a) pore filled with ettringite, showing mortar dissolution and infiltration through the brick; (b) ettringite needle-shaped crystals.

Tables

Table I. Ancient brick samples, historic building of provenance, conservation environment and architectonic structure attribution.

Table II. Porosity and pore size distribution evolution of ancient Toledo bricks.

Table III. Grain sizes of clays from ancient quarries of Toledo City.

Table IV. Average analytical data from Torcon, Guajaraz and Castrejon reservoirs, between 1987-2000.

Table V. Physicomechanical properties evolution of ancient Toledo bricks and their experimental replica bricks manufactured with original raw clays and fired at similar temperature.

Table I

Brick sample	Origin (Historical Building)	Brick Age (century)	Construction Period	Conservation environment	Location in building	Architectonic structure
DIP	Provincial Council Palace (Diputacion)	XIX	Modern	Outdoor wall	Inner courtyard	Brick wall under a window
CG3	Greco Residence (Casa del Greco)	XIV-XV	Islamic-Mudejar	Aerial / Indoor wall	Cellar	Corner of a supporting arch
CG2		XIII-XIV				Brick wall
AL3	Toledo Fortress (Alcazar)	XII-XIII	Mudejar Romanesque	Burial	Top of a buried brick wall with lime mortar. The wall forms part of an arch	
AL2						

Table II

Ancient Brick (AB)	Experimental Replica Brick (ERB)		Total porosity 0.01-110 µm (%)		Δ total porosity 0.01-110 µm (%)	Δ Pores < 0.316 µm (%)	Δ Pores 0.316-3.16 µm (%)	Δ Pores 31.6-110µm (%)
	Clay	Firing	AB	ERB	AB	AB	AB	AB
DIP	EC6	900ºC	37.6	39.7	-2.1	42.96	-41.68	-0.89
AL3	EC6	700ºC	24.9	33.5	-8.6	15.07	-14.96	0.60
CG2	SB4	800ºC	32.1	38.7	-6.6	44.57	-42.15	-0.66
CG3			27.5		-11.2	26.63	-28.96	2.79
AL2	SB4	700ºC	26.9	37.3	-10.4	25.43	-26.46	0.89

Table III

Clays		SB4 weight (%)		EC6 weight (%)	
		Total	**Fractions**	**Total**	**Fractions**
Pebble fraction	20mm-10mm	1.60		-	
Gravel fraction 10mm-2mm	10-8mm. (-3 ∅)	2.86	-	0.81	9.04
	8-4mm. (-2∅)		37.42		11.17
	4-2mm. (-1∅)		62.57		78.78
Sand fraction 2mm-0.063mm	1.414mm. (-0.5∅)	37.60	4.68	32.03	1.89
	1.000mm. (0.0∅)		3.07		2.67
	0.707mm. (+0.5∅)		3.69		2.82
	0.500mm. (+1.0∅)		3.23		3.25
	0.354mm. (+1.5∅)		4.80		3.92
	0.250mm. (+2.0∅)		10.18		5.04
	0.176mm. (+2.5∅)		18.95		5.13
	0.125mm. (+3.0∅)		24.69		8.23
	0.088mm. (+3.5∅)		13.31		11.14
	0.063mm. (+4.0∅)		13.35		55.86
Clay/silt fraction	<0.063mm	79.53		76.44	

Table IV

Non treated water	Castrejon reservoir				Torcon and Guajaraz reservoirs
Dates	**1987-1988**	**1989-1990**	**1991-1992**	**1993-1994**	**1995-1996**
T (ºC)	14.05	14.95	13.91	13.7	14.3
pH	7.6	7.01	7.05	7.4	7.56
$SO4^{=}$ (mg/l)	426.6	453.5	416.4	442.7	359.0

Table V

Ancient Brick (AB)	Experimental replica Brick (ERB)		Bulk density (g/cm^3)		Ultrasounds, v_P (km/s)		Variation of ultrasounds, Δv_P (km/s)	Variation of compression stregth, $\Delta\sigma_c$ (Mpa)
	Clay	**Firing**	**AB**	**ERB**	**AB**	**ERB**	**AB**	AB
DIP	**EC6 – 900ºC**		1.7	1.6	3.38 ± 0.19	1.83 ± 0.07	1.55	21.68
AL3	**EC6 – 700ºC**		1.7	1.7	2.78 ± 0.07	1.52 ± 0.09	1.26	12.21
CG2	**SB4 – 800ºC**		1.5	1.6	2.51 ± 0.34	2.24 ± 0.05	0.28	3.94
CG3			1.6		2.90 ± 0.21		0.66	9.22
AL2	**SB4 – 700ºC**		1.6	1.5	2.52 ± 0.11	1.56 ± 0.12	0.97	13.57

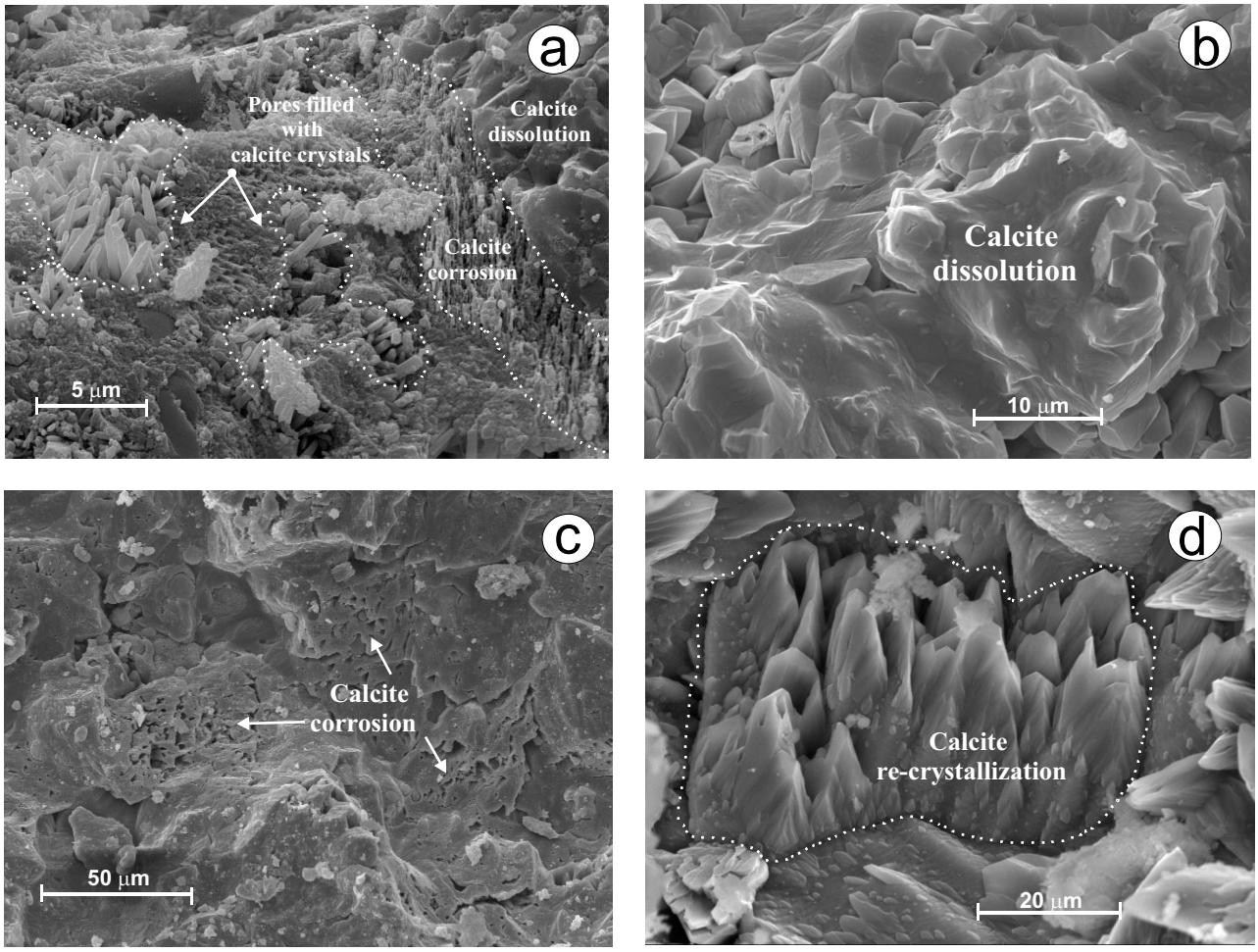

Figura 1
Lopez-Arce et al.

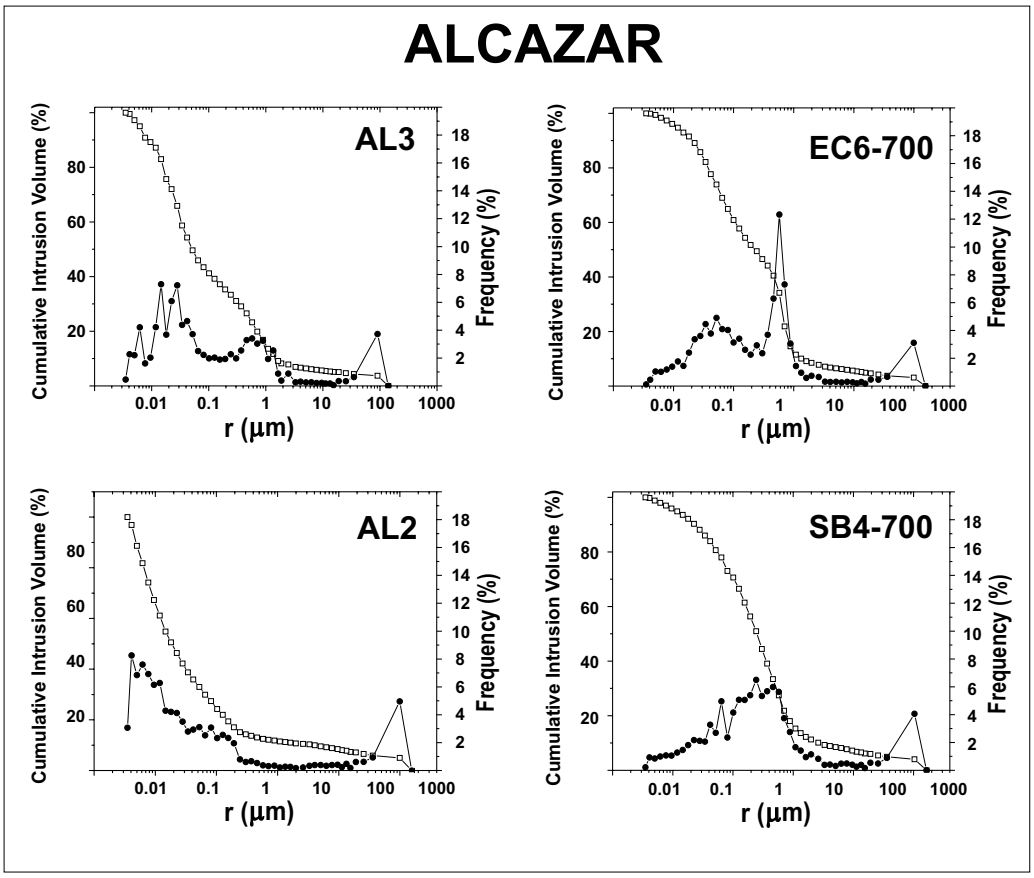

Figure 2 Lopez- Arce et al.

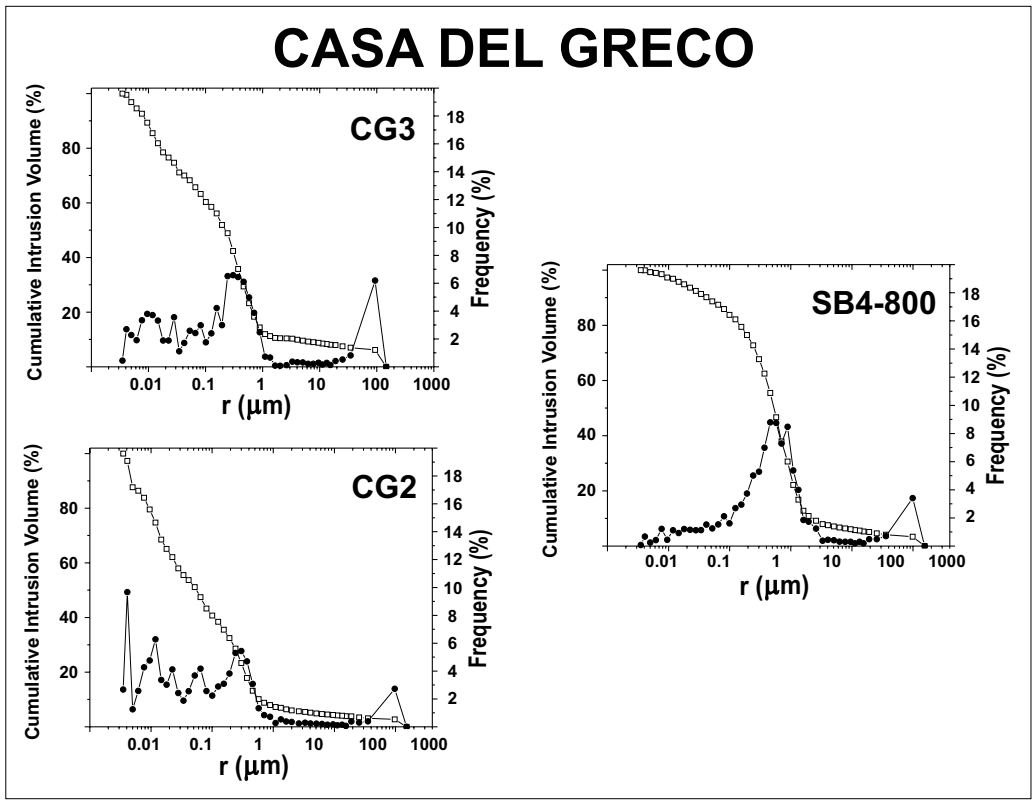

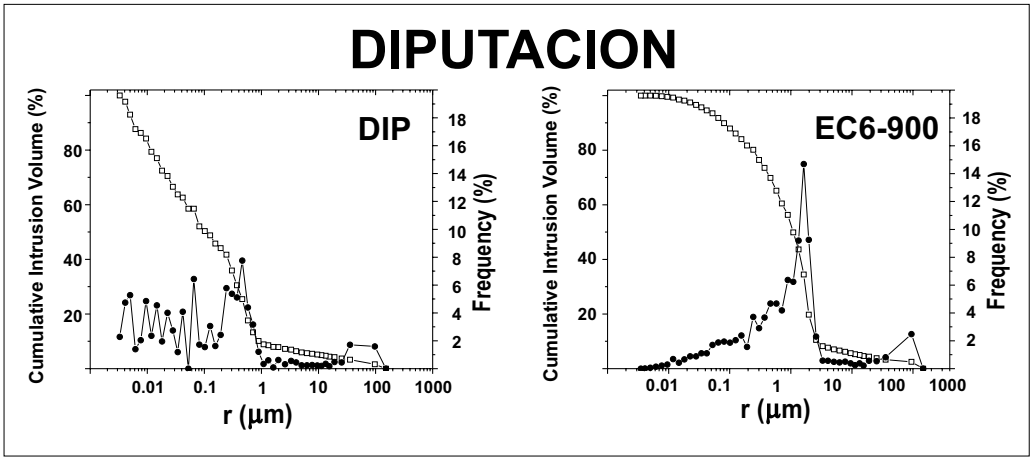

Figure 3 Lopez- Arce et al.

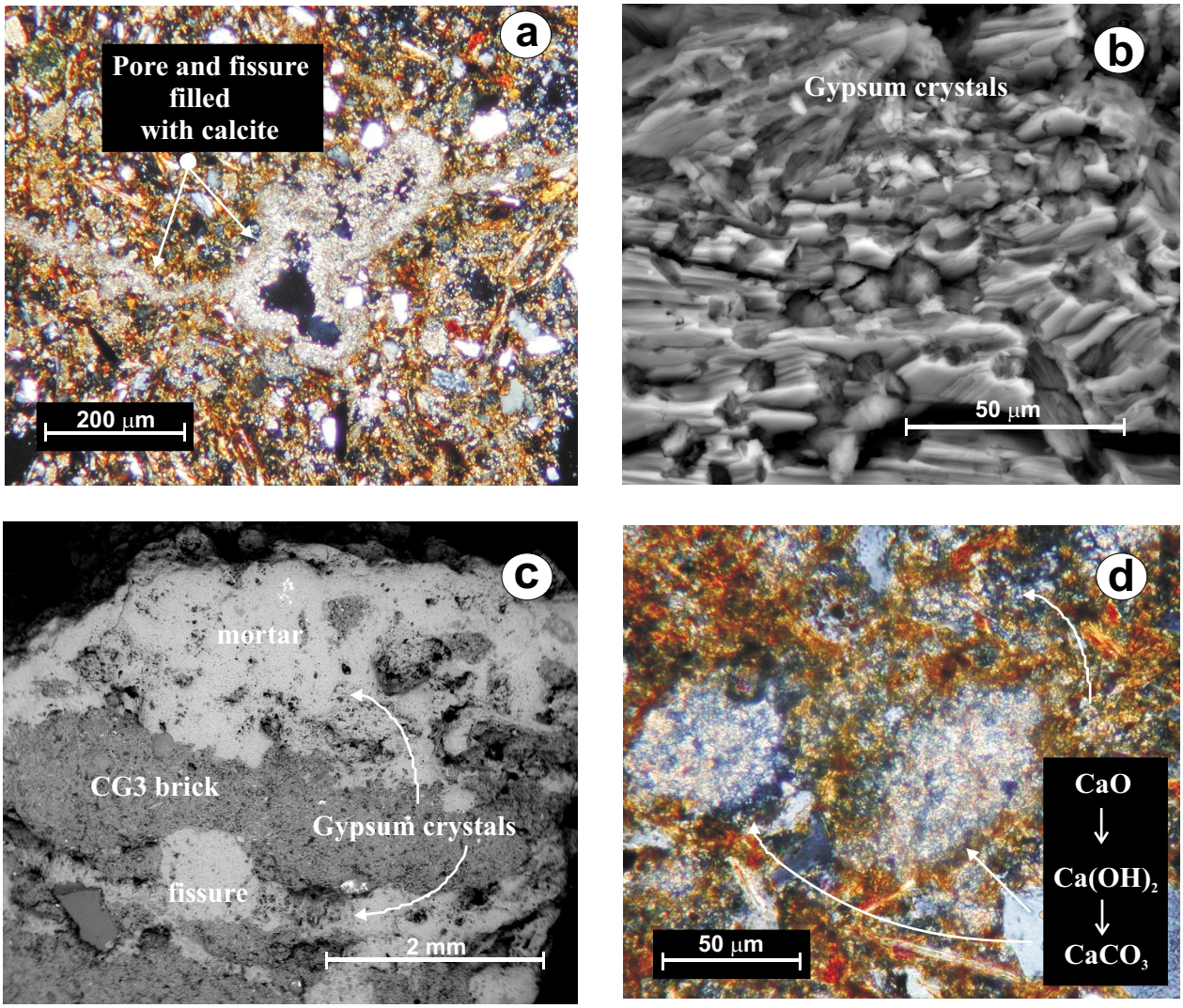

Figure 4
Lopez-Arce et al.

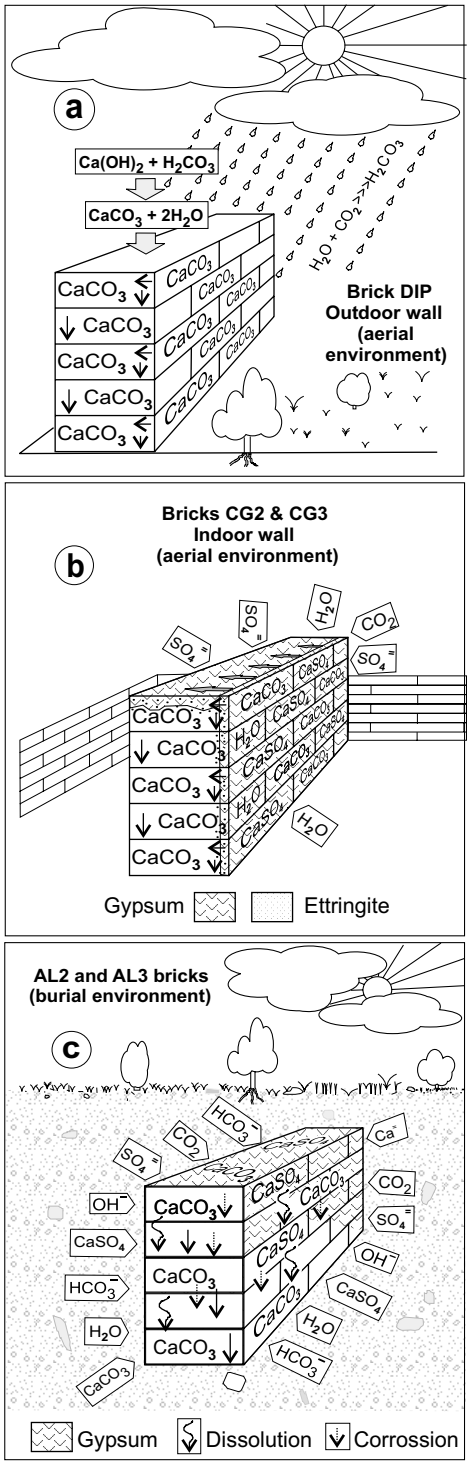

Figure 5.- Lopez-Arce et al.

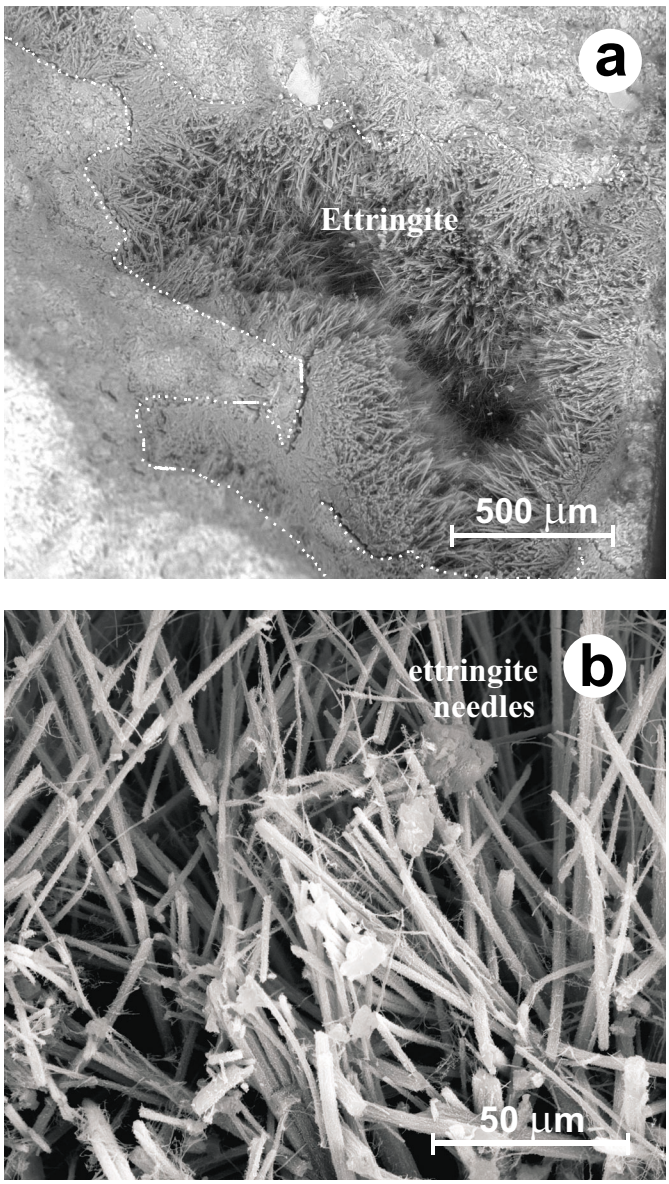

Figure 6
Lopez-Arce et al.